

Analytical and Case Studies of a Sandwich Structure using EulerBernoulli Beam Equation

Hui Xue¹, H. Khawaja^{2,*}

¹Master Student, Department of Computer Science and Computational Engineering, UiT The Arctic University of Norway, Narvik, Norway.

² Associate Professor, Department of Engineering and Safety, UiT The Arctic University of Norway, Tromsø, Norway.

* *Corresponding Author.* hassan.a.khawaja@uit.no

Abstract. This paper presents analytical and case studies of sandwich structures. In this study, the Euler–Bernoulli beam equation is solved analytically for a four-point bending problem. Appropriate initial and boundary conditions are specified to enclose the problem. In addition, the balance coefficient is calculated and the Rule of Mixtures is applied. The focus of this study is to determine the effective material properties and geometric features such as the moment of inertia. The effective parameters help in the development of a generic analytical correlation for complex sandwich structures from the perspective of four-point bending calculations. The case study is built for a sandwich structure made of two materials; Aluminum and Steel. This case is solved using MATLAB®. The main outcomes of the Al-Steel sandwich structure are the maximum lateral displacements and longitudinal stresses varying with number of sandwich layers.

1 Introduction

The EulerBernoulli beam theory states that stresses vary linearly with the distance from the neutral axis [1, 2]. The classic formula for determining the longitudinal stress in a beam, as shown in Figure 1 under simple bending, is given in Equation (1.1):

$$\sigma_x = \frac{M|c|}{I} \quad (1.1)$$

where σ_x is the longitudinal stress in Pa, M is the moment about the neutral axis in Nm, c is the perpendicular distance from the neutral axis in m and I is the second moment of area about the neutral axis in m^4 .

²⁰¹⁰ **Mathematics Subject Classification**

Keywords: Euler–Bernoulli beam equation, sandwich structures, four-point bending, MATLAB®

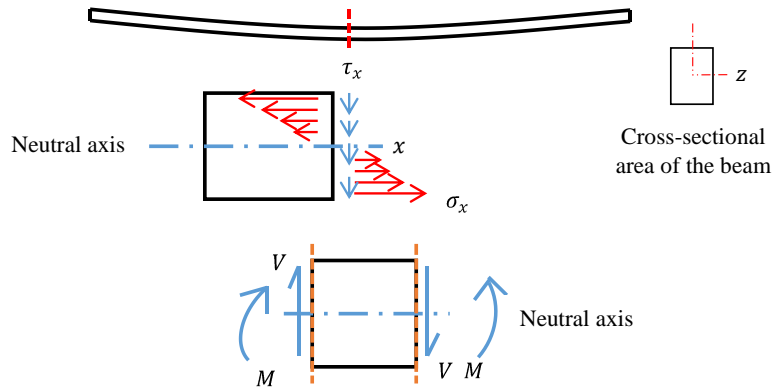


Fig. 1 Longitudinal stress (σ_x), shear stress (τ_x), shear force (V) and bending moment (M) in a beam

Deflection in the beam is shown in Figure 2 in a bending beam, the strain can be expressed by the radius of the neutral axis and the distance of the surface from the neutral axis. A correlation can be written as shown in Equation (1.2):

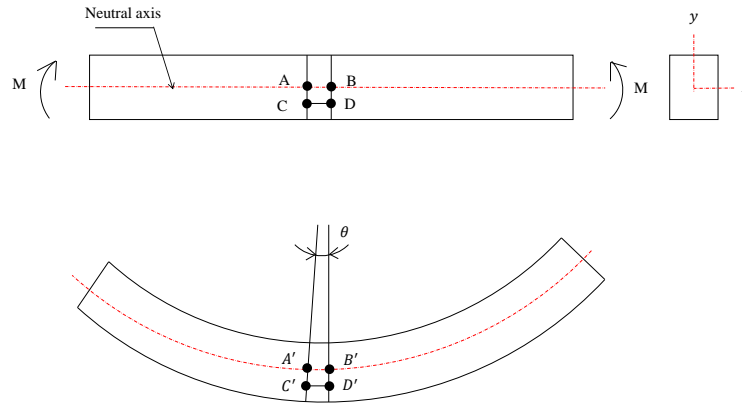


Fig. 2 Longitudinal strain(ϵ_x) in a bending beam

$$\frac{C'D'}{A'B'} = \frac{(R+c)\theta}{R\theta} = \frac{R+c}{R} \quad (1.2)$$

where R is the radius of the neutral axis, c is the distance from the neutral axis and θ is the slope in radians.

Thereafter, the strain ϵ_x at layer at $C'D'$ is shown in Equation (1.3), where the line CD is in the original layer so that the length $CD = AB$.

$$\epsilon_x = \frac{C'D' - CD}{CD} = \frac{C'D' - AB}{AB} = \frac{C'D'}{AB} - 1 \quad (1.3)$$

Since $A'B'$ and AB are on the neutral axis, there will no change in length; hence, Equation (1.4) is written as:

$$A'B' = AB \quad (1.4)$$

By substituting Equation (1.2) in Equation (1.3), Equation (1.5) can be written:

$$\epsilon_x = \frac{c}{R} \quad (1.5)$$

Since the beam is only subject to moments and it is in static equilibrium, the forces across the cross-section surface are entirely longitudinal (Fig. 3). The force on each small area in the cross-sectional area is given by Equation (1.6):

$$\Delta P = \sigma_x \cdot b \cdot dy \quad (1.6)$$

where σ_x is the longitudinal stress in Pa, b is the width of the beam in m, and dy is the differential in the y direction.

This result in moment is shown in Equation (1.7):

$$\Delta M = c \cdot (\sigma_x \cdot b \cdot dy) \quad (1.7)$$

where c is the perpendicular distance from the neutral axis in m.

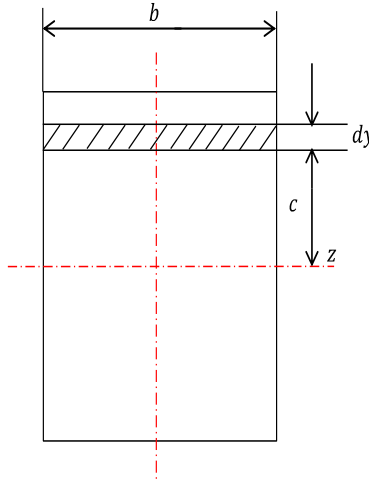


Fig. 3 Bending moment in the cross-sectional area of a beam

By summing the moment over the complete cross-sectional area, Equation (1.8) is given as:

$$M = \Sigma(\sigma_x \cdot c \cdot b \cdot dy) \quad (1.8)$$

Considering the elasticity of the material, using Hooke's law [3], Equation (1.9) is given as:

$$\sigma_x = E\varepsilon_x \quad (1.9)$$

where E is Young's modulus in Pa .

By substituting Equation (1.5) in Equation (1.9), σ_x can be re-written in Equation (1.10):

$$\sigma_x = E \frac{c}{R} \quad (1.10)$$

Figure 4 shows the shape of the neutral axis when the beam is bending.

As it is known, when the angle is very small, $\tan \theta = \frac{dy}{dx}$ can be written as $\theta = \frac{dy}{dx}$. By the definition of θ in radians ($\theta = \frac{s}{R}$, where s is length of arc and R is radius), since ds is very small so $dx = ds$, resulting in Equation (1.11):

$$\frac{1}{R} = \frac{d\theta}{ds} = \frac{d\theta}{dx} = \frac{d^2y}{dx^2} \quad (1.11)$$

By substituting Equation (1.10) and Equation (1.11) into Equation (1.8), Equation (1.12) is given as:

$$M = \frac{E}{R} \sum c^2 b \cdot dy = \frac{E}{R} \cdot I \quad (1.12)$$

where I is the moment of inertia in (m^4).

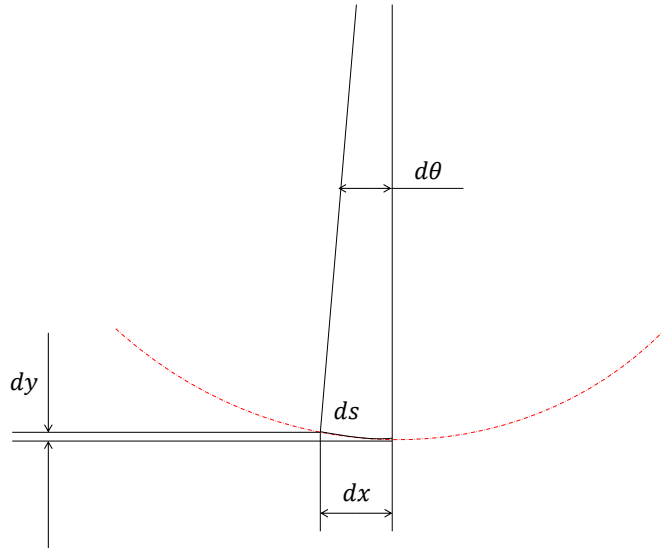


Fig. 4 Shape of neutral axis of a bending beam

By substituting Equation (1.11) in Equation (1.12), Equation (1.13) is derived as shown:

$$\frac{d^2y}{dx^2} = \frac{M}{EI} \quad (1.13)$$

Since it is known that $\theta = \frac{dy}{dx}$, Equation (1.13) can be rewritten in the form of Equation (1.14):

$$\theta = \int \frac{M}{EI} dx \quad (1.14)$$

In the end, the displacement y can be derived as shown in the form of Equation (1.15):

$$y = \int \theta dx = \iint \frac{M}{EI} dx \quad (1.15)$$

These equations [4] will later be applied to derive the correlation of displacement in the four-point bending beam.

In four-point bending [5, 6], a total force is applied to two locations at equal distance from the supports placed at two ends of the beam, as shown in Fig. 5. The resulted shear force and the bending moment are also shown in Fig. 5.

The advantage of four-point bending is that the moment is constant in the middle of the beam, however, it is function of x at both ends [7] as shown in Equation (1.16):

$$\begin{aligned} M(x) &= \frac{Px}{2} & 0 \leq x \leq L_1 \\ M &= \frac{PL_1}{2} & L_1 \leq x \leq (L - L_1) \\ M(x) &= \frac{P(L-x)}{2} & (L - L_1) \leq x \leq L \end{aligned} \quad (1.16)$$

where P is the total load in four-point bending in N , L_1 is the distance between the supporting points and the loading points on each side in m , and L is the distance between the supports in m as shown in Fig. 5.

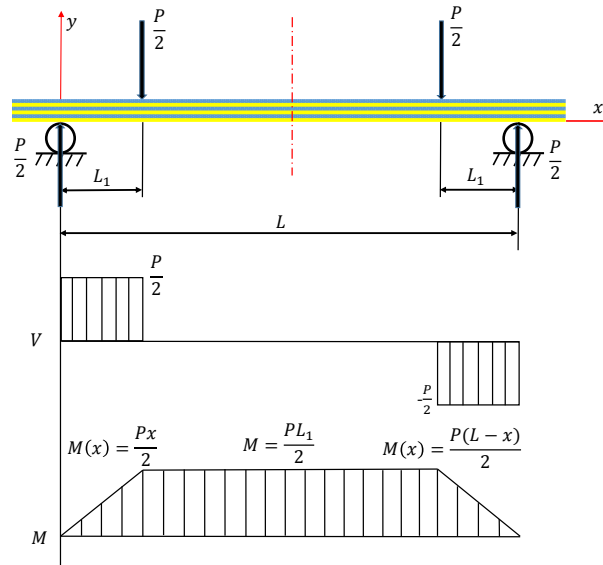


Fig. 5 Bending moment (M) and shear force (V) diagrams of a four-point bending beam

By substituting Equations (1.16) in Equations (1.14) and (1.15), the following correlations can be derived as shown in Equations (1.17) to (1.22).

When $0 \leq x \leq L_1$ and $M = \frac{Px}{2}$,

$$\theta_1 = \frac{Px^2}{4EI} + C_1 \quad (1.17)$$

$$\delta_1 = \frac{Px^3}{12EI} + C_1x + C_2 \quad (1.18)$$

When $L_1 \leq x \leq (L - L_1)$ and $M = \frac{PL_1}{2}$,

$$\theta_2 = \frac{PL_1x}{2EI} + C_3 \quad (1.19)$$

$$\delta_2 = \frac{PL_1x^2}{4EI} + C_3x + C_4 \quad (1.20)$$

When $(L - L_1) \leq x \leq L$ and $M = \frac{P(L-x)}{2}$,

$$\theta_3 = -\frac{Px^2}{4EI} + \frac{PLx}{2EI} + C_5 \quad (1.21)$$

$$\delta_3 = -\frac{Px^3}{12EI} + \frac{PLx^2}{4EI} + C_5x + C_6 \quad (1.22)$$

Since we have six unknowns $C_1, C_2, C_3, C_4, C_5,$ and C_6 we need atleast six boundary conditions (BCs) to solve the equations to get the lateral displacement δ and angular displacement θ . The BCs are given in Equations (1.23) to (1.27).

$$x = 0, \quad \delta_1 = 0 \quad (1.23)$$

$$x = L_1, \quad \delta_1 = \delta_2, \quad \theta_1 = \theta_2 \quad (1.24)$$

$$x = \frac{L}{2}, \quad \theta_2 = 0 \quad (1.25)$$

$$x = L - L_1, \quad \delta_2 = \delta_3, \quad \theta_2 = \theta_3 \quad (1.26)$$

$$x = L, \quad \delta_3 = 0 \quad (1.27)$$

By solving the equations [8], the following results of lateral and angular displacements are obtained, as shown in Equations (1.28) to (1.33),

$$\theta_1 = \frac{Px^2}{4EI} + \frac{PL_1^2}{4EI} - \frac{PL_1L}{4EI} \quad (0 \leq x \leq L_1) \quad (1.28)$$

$$\delta_1 = \frac{Px^3}{12EI} + \frac{PL_1^2x}{4EI} - \frac{PL_1Lx}{4EI} \quad (0 \leq x \leq L_1) \quad (1.29)$$

$$\theta_2 = \frac{PL_1x}{2EI} - \frac{PLL_1}{4EI} \quad (L_1 \leq x \leq (L-L_1)) \quad (1.30)$$

$$\delta_2 = \frac{PL_1x^2}{4EI} - \frac{PLL_1x}{4EI} + \frac{PL_1^3}{12EI} \quad (L_1 \leq x \leq (L-L_1)) \quad (1.31)$$

$$\theta_3 = -\frac{Px^2}{4EI} + \frac{PL}{2EI} - \frac{PL_1^2}{4EI} - \frac{PL^2}{4EI} + \frac{PLL_1}{4EI} \quad ((L-L_1) \leq x \leq L) \quad (1.32)$$

$$\delta_3 = -\frac{Px^3}{12EI} + \frac{PLx^2}{4EI} - \frac{PL_1^2x}{4EI} - \frac{PL^2x}{4EI} + \frac{PLL_1x}{4EI} + \frac{PL^3}{12EI} + \frac{PL_1^2L}{4EI} - \frac{PL^2L_1}{4EI} \quad ((L-L_1) \leq x \leq L) \quad (1.33)$$

where L is the distance between the supports, P is the total load of four-point bending, E is the Young's modulus and I is the moment of inertia.

In this study, a beam is analyzed by overlaying two different materials together to form a sandwich structure. Each layer of the material is uniformly distributed throughout and perfectly bonded, free of voids. The lamina is initially in a stress-free state (no residual stresses) and behaves as linear elastic material.

2 Analytical study

Stress calculations in the beam are performed with respect to the neutral axis. The neutral axis of the beam goes through the centroid of its cross-section [9]. The centroid can be calculated using correlations given in Equations (2.1) to (2.3):

$$C_z = \frac{\int z dA}{A} \quad (2.1)$$

$$C_y = \frac{\int y dA}{A} \quad (2.2)$$

$$A = \int f(z) dz, \quad y = f(z) \quad (2.3)$$

where C_z , C_y are the coordinates of the centroid; A is the area; z , y are the values of the z -coordinate and y -coordinate, respectively; $f(z)$ is a function which describes the shape. Since the beam is symmetric, C_z , the coordinate of the centroid on the z -axis, is in the center.

In this study, the beam is made of two different materials with thicknesses t_1 and t_2 and areas A_1 and A_2 , respectively, as shown in Fig. 6 (a). The number of sandwiched layers was analyzed, as shown in Fig.6 (b), (c) and (d). In these samples, the total thickness was kept constant and the individual material thicknesses were divided equally by the number of sandwiched layers, s ; for example, $s = 1$ for Fig. 6 (a), $s = 2$ for Fig.6 (b) and $s = 3$ for Fig. 6 (c).

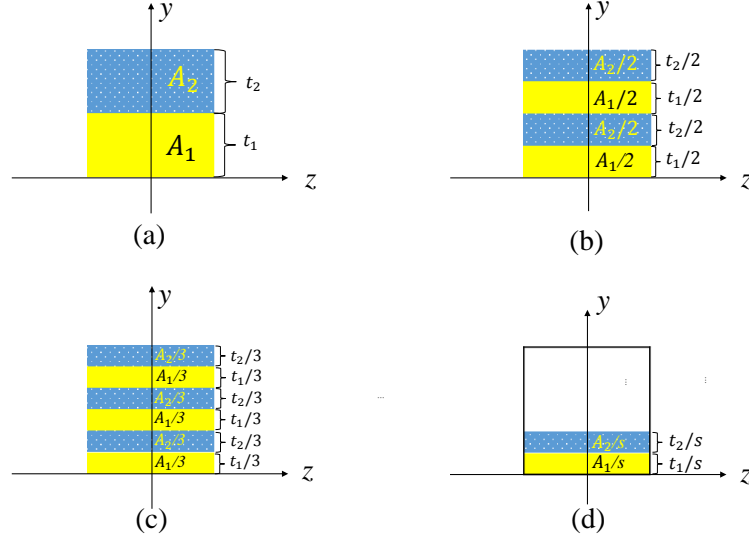


Fig. 6 The cross-sectional area of a beam with different numbers of sandwiched layers

It is valid to assume that, under tensile loading, the Young's modulus E of the beam with total cross-sectional area A can be described as shown in Equation (2.4):

$$E = E_1 \frac{A_1}{A} + E_2 \frac{A_2}{A} \quad (2.4)$$

where E_1 and E_2 are Young's moduli of different materials with the respective net cross-sectional areas, A_1 and A_2 , respectively.

This beam contains two kinds of different materials. When it is bending, different materials have different stiffness because of the different Young's modulus, E . Therefore, the Rule of Mixtures [10] is introduced to find the combined material properties.

One of the methods of analyzing the composite beams is to use an equivalent area to represent the increase (or decrease) in stiffness. Therefore, it is important to bring in the conception of the balance coefficient, n [11]. The new equivalent cross-section is assumed to be made completely from the first material, and the balance coefficient, n is multiplied by the area of the second material for scaling the stiffness difference, as shown in Fig. 7.

The expansion factor, also known as the balance coefficient n , is given in Equation (2.5):

$$n = \frac{E_2}{E_1} \quad E_1 > E_2 \text{ (assumed)} \quad (2.5)$$

The location of the centroid and the moment of inertia change because of the difference in the Young's moduli. The new value of centroid, C_y , is calculated as shown in Equation (2.6):

$$C_y = \frac{A_1 \cdot \sum D_i + n A_2 \cdot \sum D_{i+1}}{s \cdot (A_1 + n A_2)} \quad (2.6)$$

where $i = 1, 3, 5, 7, \dots, 2s - 1$, D_i and D_{i+1} are the centroid coordinates of each layer and calculated as shown in Equations (2.7) to (2.10):

$$D_1 = \frac{t_1}{2s} \quad (2.7)$$

$$D_2 = \frac{t_1}{s} + \frac{t_2}{2s} \quad (2.8)$$

$$\vdots$$

$$D_i = D_{i-2} + \frac{t_1}{s} + \frac{t_2}{s}, \quad \text{when } s \geq 2 \quad (2.9)$$

$$D_{i+1} = D_{i-1} + \frac{t_1}{s} + \frac{t_2}{s}, \quad \text{when } s \geq 2 \quad (2.10)$$

The moment of inertia of each layer can be calculated using the parallel axis theorem [12, 13], as shown in Equation (2.11):

$$I = I_{N,A} + y^2 A \quad (2.11)$$

where I is the moment of inertia for each layer, $I_{N,A}$ is the local moment of inertia of the layer, y is the distance from the neutral axis, and A is the cross-sectional area of the layer.

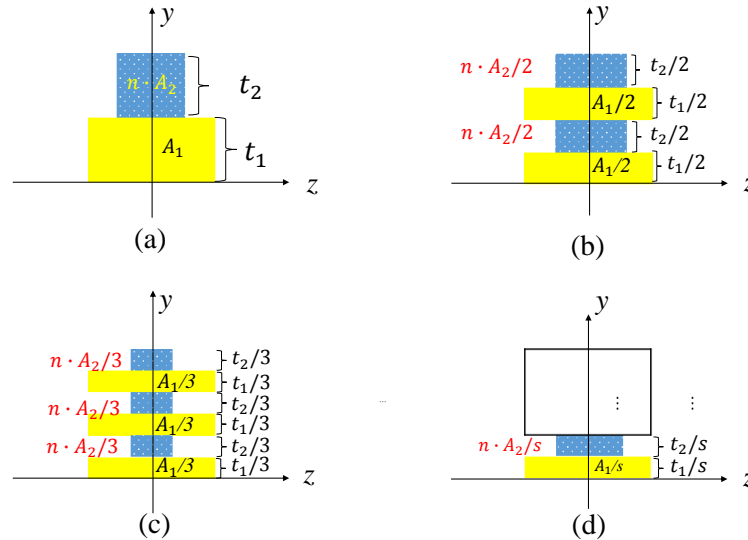


Fig. 7 Applying balance coefficient to scale the areas

All the moment of inertia terms can then be added together to calculate the total moment of inertia I_t of the lamina, as shown in Equation (2.12):

$$I_t = \sum (I_1, I_2, \dots, I_{2s-1}, I_{2s}) \quad (2.12)$$

where $I_1, I_2, \dots, I_{2s-1}, I_{2s}$ are given in Equations (2.13) to (2.16):

$$I_1 = \frac{b \cdot \left(\frac{t_1}{s}\right)^3}{12} + b \cdot \frac{t_1}{s} \cdot (D_1 - C_y)^2 \quad (2.13)$$

$$I_2 = \frac{n \cdot b \cdot \left(\frac{t_2}{s}\right)^3}{12} + n \cdot b \cdot \frac{t_2}{s} \cdot (D_2 - C_y)^2 \quad (2.14)$$

$$\vdots$$

$$I_{2s-1} = \frac{b \cdot \left(\frac{t_1}{s}\right)^3}{12} + b \cdot \frac{t_1}{s} \cdot (D_{2s-1} - C_y)^2, \quad \text{when } s \geq 2 \quad (2.15)$$

$$I_{2s} = \frac{n \cdot b \cdot \left(\frac{t_2}{s}\right)^3}{12} + n \cdot b \cdot \frac{t_2}{s} \cdot (D_{2s} - C_y)^2, \quad \text{when } s \geq 2 \quad (2.16)$$

where t_1 and t_2 are the thicknesses of material 1 and material 2, s is half of the number of layers of the beam (number of sandwiches), b is the width of the material 1, n is the balance coefficient, and C_y is the position of the neutral axis of the composite beam, as given in Equation (2.6).

The longitudinal stresses can also be determined from the basic beam bending equation [14], as given in Equation (1.1). The longitudinal stresses in each layer are given in Equations (2.17) and (2.18):

$$\sigma_{x,1} = \frac{M|y - C_y|}{I_t} \quad (2.17)$$

$$\sigma_{x,2} = \frac{nM|y - C_y|}{I_t} \quad (2.18)$$

where $\sigma_{x,1}$ and $\sigma_{x,2}$ are the longitudinal stresses in the first material and the second material, respectively, and y is the position based on the reference axis (placed at the bottom of the sample), the total moment of inertia I_t , n is the balance coefficient and M is the bending moment. Please note that the positive value of $(y - C_y)$ indicates compressive longitudinal stresses and negative value of $(y - C_y)$ indicates tensile longitudinal stresses.

Similarly, deflection and angles can be calculated using Equations (1.28) to (1.33) by substituting the lamina's Young's modulus and moment of inertia.

The maximum deflection is in the center at $x = \frac{L}{2}$ and can be calculated by substituting the value of x in Equation (1.31). The maximum deflection δ_{\max} is given in Equation (2.19):

$$\delta_{\max} = \delta_{\text{center}} = \frac{PL_1}{48EI_t} (4L_1^2 - 3L^2) \quad (2.19)$$

where δ_{center} is the deflection in the centre, L is the total length, L_1 is the distance between the support point and the loading point, E is the combined Young's modulus (Equation (2.4)) and I_t is the total moment of inertia about the neutral axis (Equation (2.12)).

3 Case study

A case study is devised to demonstrate the analytical model discussed above. the size of the beam was decided as (420 mm) length \times (50 mm) width \times (50 mm) height [5]. In this cases study, a sandwich structure is built using two different materials: Aluminum and Steel. The distance between an inner and an outer support is chosen to be one third of the distance between the two outer supports [5]. The values of parameters used in this case study are given in Table 1.

In this study the behavior of both material is assumed to be linear elastic isotropic [12] and at room temperature pressure (RTP). The material properties of both Aluminum and Steel are given in Table 2.

Description	Variable	Units	Value
Distance between the two support points on the beam	L	mm	420
Distance between the support and the load points	L_1	mm	140
Total Thickness of the beam	t	mm	50
Total Thickness of the Aluminum	t_1	mm	30
Total Thickness of the Steel	t_2	mm	20
Width of the beam	b	mm	50
Loads	P	N	100

Table 1 Description and values of the parameters for four-point bending

Mechanical Property	Aluminum	Steel
Young's Modulus (<i>GPa</i>)	$E_1 = 69$	$E_2 = 207$
Shear Modulus (<i>GPa</i>)	25	83
Poisson's Ratio (<i>dimensionless</i>)	0.33	0.3

Table 2 Mechanical material properties of Aluminum and Steel [5]

The case study is focused on the number of layers in the sandwich structure. It is to be noted that the net volume of each material was kept constant when number of layers were changed (as shown in Figure 7).

The lateral displacement under four-point bending can be calculated using Equations (1.29), (1.31) and (1.33). Using the parameters and properties provided in Table 1 and Table 2, the lateral displacement is plotted against the longitudinal direction under four-point loading as shown in Figure 8. The Figure 8 shows the deformation for number of sandwiched layers: $s = 2$, $s = 5$, and $s = 20$. It can be noticed that there is no significant variation in the lateral displacement profiles with the change of number of sandwiched layers.

The maximum longitudinal stress can be calculated in a sandwich structure for both materials (i.e. Aluminum and Steel) using Equations (2.17) and (2.18). Using the parameters and properties provided in Table 1 and Table 2, the maximum stress in both materials is calculated under four-point loading by varying the number of layers. The obtained results are given in Figure 9.

With the increase of sandwiched layers the neutral axis shifts and so as the value of the second moment of inertia changes. Since the longitudinal stress is function of the position of the neutral axis and the second moment of inertia, therefore it changes as well. This results in variation in the longitudinal stress values. As shown in Figure 8, the maximum longitudinal stress in softer material (i.e. Aluminum in this case) drops. An opposite trend can be noticed for the stiffer material (i.e. Steel in this case). The variation in maximum longitudinal stresses are higher when the number of sandwiched layers is less than 10. When the number of the sandwiched layers reaches to 20, the variation becomes small.

Similarly, the maximum lateral displacement can be calculated using Equation (2.19). Using the parameter values and mechanical properties provided in Table 1 and 2, the maximum lateral displacement under four-point bending can be calculated by varying the number of layers. The obtained results are given in Figure 10.

In this particular case, the maximum variation in the maximum lateral displacement is around 4%. Therefore, it can be deduced that the maximum lateral displacement does not vary significantly by changing the number of layers, however, as shown in Figure 10, the maximum lateral displacement value increases with the increase in the number of sandwiched layers. It can also be noticed that the

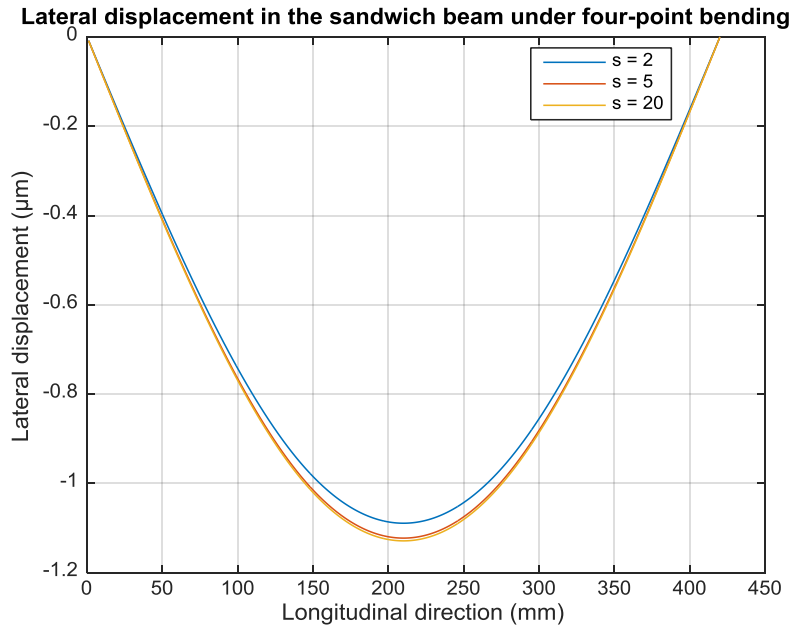


Fig. 8 Lateral displacement in the sandwich beam under four-point bending; for number of sandwiched layers: $s = 2$, $s = 5$, and $s = 20$

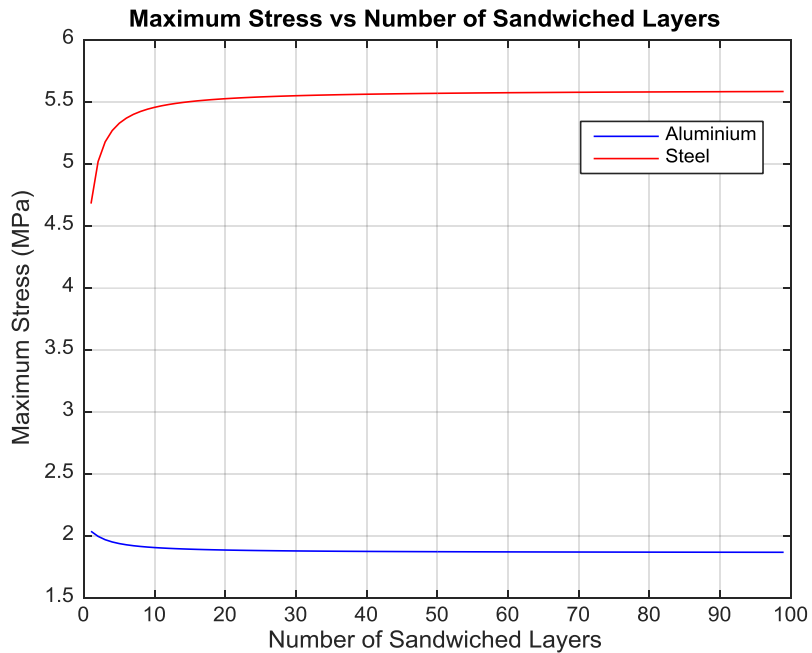


Fig. 9 Maximum longitudinal stress of the Aluminium $\sigma_{x,1}$ and Steel $\sigma_{x,2}$ in the sandwich structure varying with number of sandwiched layers: $s = 2$ to $s = 100$

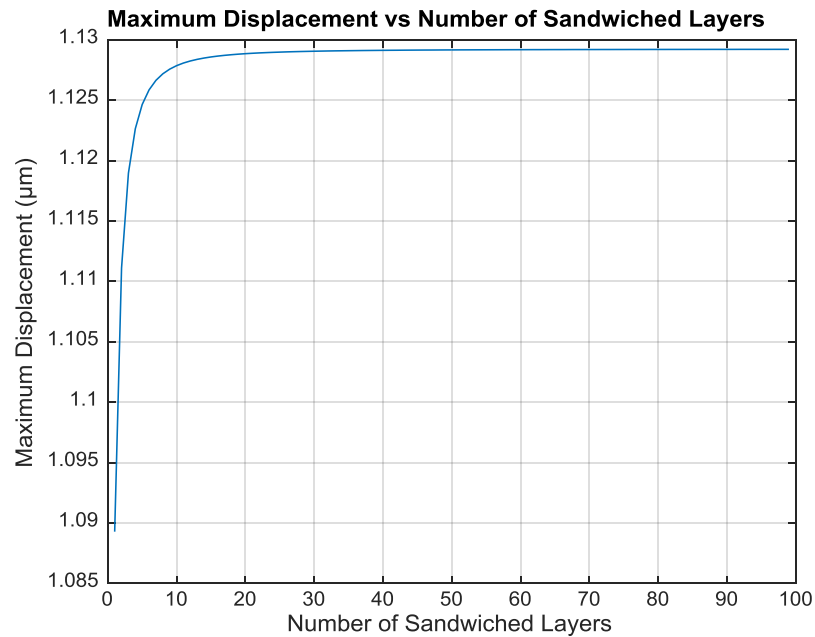


Fig. 10 Trend of maximum deflection δ_{\max} with the number of sandwiched layers: $s = 2$ to $s = 100$

variation in maximum lateral displacement is higher when the number of sandwiched layers is less than 10 and almost negligible when numbers of layers are greater than 20.

4 Conclusion

In this study, analytical correlations for displacements and longitudinal stress are derived from the Euler–Bernoulli beam equation for a four-point bending of a sandwich structure. Appropriate initial and boundary conditions are specified to enclose the problem. The Rule of Mixtures is applied to calculate the position of the neutral axis and the moment of inertia. The resulting correlations can be used to calculate the displacements and longitudinal stresses at any point in a complex sandwich beam. The study is extended to Aluminum–Steel sandwich, where parametric values for a four-point beam are devised. Results shows that the stresses decreases in softer material and increase in stiffer material with the increase of number of sandwiched layers. In this particular case, it was found that there is less than 4% variation is the maximum lateral displacement. Results also showed that the maximum displacement increases with the increase of number of sandwiched layers.

Acknowledgements

The authors would like to acknowledge the support of Linda March from The Good English Company, UK for proofreading this work.

References

- [1] SK Park and XL Gao. Bernoulli–euler beam model based on a modified couple stress theory. *Journal of Micromechanics and Microengineering*, 16(11):2355, 2006.
- [2] Olivier A Bauchau and James I Craig. *Structural analysis: with applications to aerospace structures*, volume 163. Springer Science & Business Media, 2009.
- [3] Teodor M Atanackovic and Ardéshir Guran. *Theory of elasticity for scientists and engineers*. Springer Science & Business Media, 2012.
- [4] Hui Xue, Hassan Abbas Khawaja, and Mojtaba Moatamedi. Multiphysics design optimization for aerospace applications: Case study on helicopter loading hanger. 2014.
- [5] Jorge Carvalho Pais and John Harvey. *Four point bending*. CRC Press, 2012.
- [6] Hui Xue and Hassan Abbas Khawaja. Investigation of ice-pvc separation under flexural loading using multiphysics analysis. 10(3):247–264, 2016.
- [7] John B Wachtman, W Roger Cannon, and M John Matthewson. *Mechanical properties of ceramics*. John Wiley & Sons, 2009.
- [8] Warren Clarence Young and Richard Gordon Budynas. *Roark’s formulas for stress and strain*, volume 7. McGraw-Hill New York, 2002.
- [9] JW Welleman. Engineering mechanics: volume 2: stresses, strains, displacements. 2007.
- [10] Wole Soboyejo. *Mechanical properties of engineered materials*, volume 152. CRC press, 2002.
- [11] Russell C Hibbeler. *Statics and mechanics of materials*. Pearson Higher Ed, 2013.
- [12] Robert M Jones. *Mechanics of composite materials*, volume 193. Scripta Book Company Washington, DC, 1975.
- [13] Ovid Wallace Eshbach, Byron D Tapley, and Thurman R Poston. *Eshbach’s handbook of engineering fundamentals*. John Wiley & Sons, 1990.
- [14] Das Madan Mohan et al. *Basic Engineering Mechanics and Strength of Materials*. PHI Learning Pvt. Ltd., 2010.